ACADEMY JOURNAL OF SCIENCE AND ENGINEERING
Available online @ www.academyjsekad.edu.ng
AJSE 17 (1) 2023
Original Research

MODELING AND SIMULATION OF LAMINATE COMPOSITE MATERIALS (MILD STEEL-BULK METALLIC GLASS-DYNEEMA) FOR USE AS BALLISTIC PROTECTION

Akindapo, J. O.,[1*] Orueri, D. U.,[1] Johnson-Anamemena, N.[2] and Gideon, C.J.[1]

[1]Nigerian Defence Academy, Department of Mechanical Engineering, Kaduna
[2]Airforce Institute of Technology, Department of Mechanical Engineering, Kaduna

Abstract

In this study, laminate composite materials are numerically modeled and simulated for application as ballistic protection. Using Abaqus Explicit FEA software for the numerical study, Mild Steel, Bulk Metallic Glass (BMG), and Dyneema were used as the target laminate materials and tested against 7.62mm API bullets. The maximum Von Mises stress was 9.003E8 N/m^2 at a velocity of 275 m/s and a plate thickness of 10 mm, with an average deflection of 0.0008 m. The greatest Von Mises stress at 264 m/s was 8.689E8 N/m^2, and the deflection was 0.00078 m. At 249 m/s, the Von Mises stress was 8.538E8 N/m^2, and the deflection was 0.00074 m. At 215 m/s, the Von Mises stress was 8.510E8 N/m2, and the average deflection was 0.00068 m. Thicker targets of the same material and configuration deflect bullet kinetic energy more effectively than thin targets. The weight on the wearer increases with the thickness of the material used. The simulation demonstrated that a material with a 13mm thickness could withstand the impact of a 7.62API projectile traveling at a speed of up to 850m/s. According to NIJ Standard-0101.06, this ballistic limit satisfies the standards for Level IV armour because Level IV armour is intended to stop armour-piercing rifle rounds up to and including 30 caliber M2 AP ammunition, which has a comparable velocity range. Because level IV armour plates can only weigh a maximum of 3.6 kg, a thickness of 14mm is suggested for the design, giving it a ballistic limit more than 850m/s. The thicker the material, the higher its ballistic limit.

Keywords: Mild Steel, Dyneema, Bulk Metallic Glass, Body Armour, Ballistic Limit, Computational Techniques.

Corresponding author's e-mail: danieldakseal@gmail.com

1.0 INTRODUCTION

Due to constantly growing threats in the early years of the industrial revolution, it became necessary even for tiny armies to be adequately armed. Consequently, ballistic protection was required. The National Institute of Justice Standard [1] defines ballistic protections as protection from knife or stab threats during attacks as well as protection from bullet impact. The advancement in manufacturing methods allowed for or made it practicable to supply even massive armies with complete armour kits. Body armour consequently became effective ballistic protective equipment.

Armour designers have struggled to balance mobility and protection because mobility calls for the lightest armour while protection improves as the weight of metallic armour grows, decreasing mobility. This has sparked creativity and invention in the study of armour materials and the development of armour systems [2]. Therefore, in order to save energy and to improve mobility, the development of armour materials mostly concentrated on making current armour materials lighter. Thus, the main factors for material selection are durability, flexibility, light weight, and excellent energy absorption. As a result, textiles and composites became commonplace in modern armour [3].

A thermoplastic film is sandwiched between two layers of extended chain polyethylene filament tows to create the unidirectional laminate known as Dyneema. One of the toughest and most luxurious fiber laminates made for ballistic protection is this one [4]. With a relative density that is lower than water, it is extremely thin and among the lightest ballistic protective materials known [4]. It will aid in preventing stabs and provides effective protection from cuts and slashes. It can tolerate temperatures of up to 140 °C and retains its protective qualities at temperatures as low as -150 °C.

Due to its high strength and toughness, which make it a useful material for absorbing the energy of a bullet, mild steel is frequently employed in ballistics. When a projectile collides with mild steel, the steel deforms and absorbs the impact energy, lowering the projectile's velocity and possibly even bringing it to a stop. Mild steel is a cost-effective option for several ballistic applications because it is also a relatively affordable material. In the building of shooting range backstops, for instance, as well as in the armour plating of cars and other structures, it is frequently utilized [5].

Amorphous metals like bulk metallic glass (BMG) have recently attracted interest as promising ballistic materials. High strength and hardness, as well as the capacity to absorb energy without breaking or shattering like more conventionally fragile materials, are all characteristics of BMG. It is therefore a desirable candidate for use in armour and defense mechanisms [6].

A powerful computational tool, Abaqus FEA (Finite Element Analysis), can be utilized for a variety of engineering applications, including ballistics analysis. The capacity of Abaqus FEA to faithfully mimic the complicated behavior of materials under high strain rates, such as those experienced in ballistic hits, is crucial for ballistics analysis [7].

The behavior of a variety of materials, including metals, composites, and polymers, under different loading situations, including high-velocity impact, may be modeled and examined using Abaqus FEA. As a result, it may be used to develop and optimize armour and protection systems as well as to forecast how different parts and structures would perform in ballistics applications [8].

2.0 REVIEW OF EXISTING LITERATURE

Slepyan and Ayzenberg-Stepanenko reported theoretical and computational solutions in 1998 that described the dynamics and fracture of composite metal-fabric armour penetrated by tiny projectiles (bullets and fragments). For the nonlinear dynamics of a ply, one-dimensional and spatial axisymmetric models were compared, and their suitability for use in actual calculations was examined. A calculation tool specifically created to simulate penetration processes in real metal/fabric shields was characterized as having as its foundation a computer model for the spatial dynamics of composite armour. Based on the analysis of experimental data and energy considerations, the projectile's residual parameters after piercing the primary metal armour were determined. The Israeli Military Industries Company's actual steel-kevlar shield test data and calculation results were compared, demonstrating the formula's sufficient applicability of the tool [9].

In 2005, Madhu et al. conducted an experimental investigation to see how ceramic tiles made of 95% and 99.5% alumina would behave under normal impact from strong steel 12.7 mm AP bullets traveling at speeds between 500 and 830 m/s. Projectiles that were shattered and typical damaged targets were displayed. In each experiment, the depth of penetration was measured, and the ceramic plates' ballistic efficiency factor was calculated. The efficiency factor increased as projectile velocity increased, according to the results. The ballistic efficiency factor for a given velocity was seen to decrease for ceramic tiles of 99.5% grade and increase for ceramic tiles of 95% grade as the thickness of the tile increased. When compared to alumina with a 95% purity, higher purity alumina (99.5%) demonstrated better ballistic performance. While the 95% alumina displayed a less well-defined fracture surface, the 99.5% alumina displayed a primarily transcrystalline fracture. The same (d/t) ratio used in the 12.7 mm AP trials was also used in the 7.62 mm AP experiments, and the findings were presented [10].

In a 2009 study, Kumar et al. used numerical simulations to examine the ballistic response of laminated composite plates. Thick Kevlar/epoxy composite plates, which are frequently employed in body armour, were subjected to numerical simulations to test their ballistic response. These plates were struck at speeds ranging from 100 m/s to 1000 m/s. In order to determine an estimate for the ballistic limit velocity, energy absorbed by the plate, and contact duration, a numerical parametric study of the ballistic impact induced by cylindrical projectile was conducted. Additionally, the impact of projectile mass and diameter on ballistic limit velocity was investigated. The findings reached here were in line with experimental data reported by other researchers [11] in a positive way.

The focus of the 2011 study by Durmus et al. was on the ballistic performances of cold-rolled sheet metal plates that were 1 and 2 mm thick and 2 X 1 mm thick against 9mm standard NATO projectiles. Measurements included the projectile's velocity prior to and following perforation, the diameter of the deformed front face, the depth of the crater, and the diameter of the hole. Microscopically analyzing the fracture surfaces of the plates close to the ballistic limit. The 1 mm-thick plate had the lowest ballistic limit (97 m/s), while the 2 mm-thick plate had the highest (332 m/s). While the 2 X 1 mm-thick plate's ballistic limit dropped to 306 m/s. The projectile's typical failure mechanisms were mushrooming and flattening at low speeds and detachment from the jacket at high speeds. The target plate with a thickness of 2 mm had the highest hardness value in compliance with the ballistic restrictions. Microscopic examinations revealed that the test significantly reduced the grain size of the targets [12].

Mohamed and Ahmed conducted research in 2014 on the penetration of 23 mm hard projectiles into mild steel plates, using 500 mm square plates with 30, 50, 60, and 150mm total thicknesses. Results for ballistic limitations from experiments were compared to those from known empirical and analytical relations. Additionally, computer simulations were run to forecast the outcomes of the experiment. For the purpose of implementing simulation, erosion criteria were created. The prediction of penetration into steel plates was examined in relation to the erosion strain value for which cells were deleted. According to the numerical findings, the erosion strain value significantly affected predictions of steel plate perforation [13].

The 2015 research project by Sanusi and Akindapo examined the ballistic performance of quenched and tempered steel. Austenitization, quenching, and ultimately tempering at 600oC were given to low alloy steel. After the bullet and the heat-treated steel interacted, the failure occurrence was examined. The heat-treated steel was then shot with armour-piercing 7.62 mm calibre. The shot was fired with an 830 m/s projectile at zero degrees of obliquity. After the shot, scanning electron microscopes were used to conduct microstructural and fractographical analyses on the sample collected from the perforated region to identify the matrix phase and secondary phases. After heat treatments, it was noticed that the steels' martensitic-bainitic matrices had been tempered; a crater had developed on the steel's front side; deformed and transformed adiabatic shear bands had an impact on the crack formation and spread within the matrix; and the steels' perforation mode was the standard petalling [14].

In 2017, Chang et al. used the finite element (FE) analysis program Abaqus to study the impact reactions of a steel plate with four corners that were simply supported. This software simulates the mechanisms by which the colliding bodies interact. To document the experimental characteristics of these plates, a hammer drop test was performed. In order to evaluate the effectiveness of the traditional approach with that of Abaqus, the Navier solution was then used to examine the dynamic displacement of the specimens[15]. In order to gather the core design information for a combat vehicle platform, Chanyoung and Chongdu performed a numerical analysis on the impact response of HHAP (High Hardness Armour Plate) sequences under a 7.62 mm projectile impact in 2017. Recent research suggests that combat vehicles' ballistic protection levels should rise and that multi-hit missiles should now be able to be deflected by ballistic protection technologies. Armour-plate sequences of one or two layers with a gap of 0 mm to 2 mm between the front and rear plate were defined under the same weight and thickness in order to explore the ballistic-impact characteristics. Ballistics tests and an analysis of the single plate under the impact of a 7.62 mm round were carried out in order to certify the accuracy of the numerical model. The performance and analysis of a numerical analysis were done using a reliable numerical model. Finally, it was established that the two-layer sequence with the 2 mm gap had the best performances in terms of impact-response acceleration, deflection effectiveness, and penetration depth [16].

Finite element analysis was used by Guodong et al. in 2020 to examine the ballistic performance of two various ceramic-based armour systems. A ceramic front layer and a Kevlar-29 composite backing layer made up the initial design's bi-layer armour. TThe second design had a Kevlar-29 composite backing layer and a ceramic-filled honeycomb front layer. The commercial program Abaqus/Explicit was used to create 3D finite element models. By contrasting the models with experimental data from various sources, the models were found to be valid. A 5.5 g, ogival-nosed bullet made of hardened steel 4340 was used to simulate single-hit and double-hit impacts. Comparing the two designs' ballistic capabilities in terms of ballistic resistance and penetrating methods. It was discovered that the second armour design's ballistic performance was significantly impacted by the honeycomb's inclusion. The fracture was contained in a small area by the cell walls, which stopped the stress wave's progression. The ballistic limit of the second armour design in a single-hit impact decreased significantly but the resistance to a second hit did not decrease [17].

3.0 GOVERNING ANALYTICAL EQUATIONS

3.1 Constitutive Model

In order to define the material behaviour of mild steel target and armour piercing projectile the Johnson-Cook elasto-viscoplastic material model available in Abaqus finite element code was employed. The material model includes the effect of linear thermo-elasticity, yielding, plastic flow, isotropic strain hardening, strain rate hardening, softening due to adiabatic heating and fracture effects. The equivalent Von-Mises stress, $(\bar{\sigma})$ of the Johnson-Cook model is defined as [18];

$$\bar{\sigma}\left(\bar{\varepsilon}\rho l, \bar{\varepsilon}\rho \dot{l}, \hat{T}\right) = [A + B(\bar{\varepsilon}\rho l)n]\left[1 + Cln\left(\frac{\bar{\varepsilon}\dot{\rho} l}{\dot{\varepsilon_o}}\right)\right]\left[1 - \hat{T}m\right] \tag{1}$$

Where A, B, n, C and m are material parameters determined from different mechanical tests. $\bar{\varepsilon}\rho l$ is equivalent plastic strain, $\bar{\varepsilon}\dot{\rho} l$ is equivalent plastic strain rate, $\dot{\varepsilon_o}$ is a reference strain rate and $\hat{T}$ is non-dimensional temperature defined by [18];

$$\hat{T} = \frac{T - T_o}{T_{melt} - T_o}; \quad T_o \leq T \leq T_{melt} \tag{2}$$

Where T is the current temperature, T_{melt} is the melting point temperature and T_0 is the room temperature. Johnson and Cook extended the failure criterion proposed by Hancock and Mackenzie by incorporating the effect of strain path, strain rate and temperature in the fracture strain expression, in addition to stress triaxiality. The fracture criterion is based on the damage evolution wherein the damage of the material is assumed to occur when the damage parameter, ω, exceeds unity [18];

$$\omega = \sum\left(\frac{\Delta\bar{\varepsilon}\rho l}{\bar{\varepsilon}f\rho l}\right) \tag{3}$$

Where $\Delta\bar{\varepsilon}\rho l$ is an increment of the equivalent plastic strain, $\bar{\varepsilon}f\rho l$ is the strain at failure, and the summation is performed over all the increments throughout the analysis. The strain at failure is assumed to be dependent on a non-dimensional plastic strain rate, $\frac{\bar{\varepsilon}\dot{\rho} l}{\dot{\varepsilon_o}}$; a dimensionless pressure-deviatoric stress ratio, $\frac{\sigma_m}{\bar{\sigma}}$, (where σ_m is the mean stress and $\bar{\sigma}$ is the equivalent Von-Mises stress) and the non-dimensional temperature, $\hat{T}$, defined earlier in the Johnson-Cook hardening model. The dependencies are assumed to be separable and are of the form [18];

$$\bar{\varepsilon}f\rho l\left(\frac{\sigma_m}{\bar{\sigma}}, \bar{\varepsilon}\dot{\rho} l, \hat{T}\right) = \left[D_1 + D_2 exp\left(D_3\frac{\sigma_m}{\bar{\sigma}}\right)\right]\left[1 + D_4 ln\left(\frac{\bar{\varepsilon}\dot{\rho} l}{\dot{\varepsilon_0}}\right)\right]\left[1 + D_5\hat{T}\right] \tag{4}$$

Where D_1 - D_5 are material parameters determined from different mechanical tests. When the material damage occurs, the stress-strain relationship no longer accurately represents the material behaviour. The use of stress-strain relationship beyond the ultimate stress introduces a strong mesh dependency based on strain localization i.e., the energy dissipated decreases with a decrease in element size [18].

3.2 Ballistic Limit

The ballistic limit or limit velocity is the velocity required for a particular projectile to reliably (at least 50% of the time) penetrate a particular piece of material. In other words, a given projectile will generally not pierce a given target when the projectile velocity is lower than the ballistic limit [19].

The ballistic limit equation for laminates is expressed as [19];

$$V_b = \frac{\pi\Gamma\sqrt{(\rho_t)(\sigma_e)}}{4m} D^2 T \left[1 + \sqrt{1 + \frac{8m}{\pi\Gamma^2\rho_t D^2 T}}\right] \qquad (5)$$

Where;
V_b = the ballistic limit
Γ = projectile constant determined experimentally
ρ_t = the density of the laminate
σ_e = the static linear elastic compression limit
D = the diameter of the projectile
T = the thickness of the laminate
m = the mass of the projectile

Additionally, the ballistic limit for small-caliber into homogenous armour by TM5-855-1 is [19]:

$$V_l = 19.72 \left[\frac{7800 d^3 \left[\left(\frac{e_h}{d}\right) sec\theta\right]^{1.6}}{W_T}\right]^{0.5} \qquad (6)$$

Where;
V_l = the ballistic limit velocity multiplied by 0.34m/s
d = the caliber of the projectile multiplied by 0.0254m
e_h = the thickness of the homogenous armour multiplied by 0.0254m
Θ = the angle of obliquity
W_T = the weight of the projectile multiplied by 0.4kg.

The V_{50} ballistic limit is the velocity at which a specific projectile is expected to penetrate the armour half of the time. The ballistic limit of armour is most frequently conducted using the procedures of MIL-STD-662D [19].

4.0 MATERIALS, EQUIPMENT AND METHODS

4.1 Materials

The following materials were used in this research work;
i. Mild steel
ii. Bulk metallic glass
iii. Dyneema
iv. 7.62mm API Projectile

The material properties employed are reflected in the tables below;

a) Mild steel target and Projectile

Table 1: Material Properties for Mild steel target and projectile [17, 20]

Description	Mild steel (Projectile)	Mild steel (Target)
Modulus of elasticity	$210 \times 10^9 N/m^2$	$203 \times 10^9 N/m^2$
Poisson's ratio, υ	0.3	0.33
Density	$7850 Kg/m^3$	$7850 Kg/m^3$
Yield stress constant, A	$0.95 \times 10^9 N/m^2$	$304.330 \times 10^6 N/m^2$
Strain hardening constant, B	$0.725 \times 10^9 N/m^2$	$422.007 \times 10^6 N/m^2$
N	0.375	0.345
Viscous effect, C	0.015	0.0156
Thermal softening constant, M	0.625	0.87
Reference strain rate, $\acute{\varepsilon}_0$	$1 s^{-1}$	$0.0001 s^{-1}$
Melting temperature	1793K	1800K
Transition temperature	293K	293K
Fraction strain constant D1	-0.8	0.1152
D2	2.1	1.0116
D3	0.5	-1.7684
D4	0.002	-0.05279
D5	0.61	0.5262

b) Material properties of Dyneema and BMG

Table 2: Material Properties of Dyneema and BMG [21, 22]

Description (Dyneema)	Value	Description (BMG)	Value
Density	975Kg/m^3	**Density**	6800Kg/m^3
Axial tensile strength	3.6 x 10^{9}N/m^2	**Hardness (Rockwell) (Vickers)**	47 460
Axial tensile Modulus	116 x 10^{9}N/m^2	**Charpy Impact**	3.5J/m^2
Axial compressive Strength	0.1 x 10^{9}N/m^2	**Fatigue Strength**	206 Mpa @ 10^7 cycles
Axial compressive Modulus	116 x 10^{9}N/m^2	**Poisson's ratio**	0.38
Transverse tensile Strength	0.03 x 10^{9}N/m^2	**Young's modulus**	85 x 10^{9}N/m^2
Transverse Modulus	3 x 10^{9}N/m^2	**Ultimate tensile strength**	1200 x 10^{6}N/m^2
Transverse compressive strength	0.1 x 10^{9}N/m^2	**Elastic strain (% of original shape)**	1.6%
		Glass transition temperature	~425^{o}C

4.2 Equipment

The equipment used in this work was a Toshiba personal computer rated as follows;

Device Specifications

i) Device name DESKTOP-3SU5545
ii) Processor Intel® Core™ i5-4300U CPU @ 1.90GHz – 2.50GHz
iii) Installed RAM 4.00 GB
iv) System type 64-bit operating system x64-based processor

Windows Specifications

i) Edition Windows 10 Pro
ii) Version 21H2
iii) OS build 19044.1645
iv) Experience Windows Feature Experience Pack 120.2212.4170.0

The software employed in the modelling and analyses was Abaqus/CAE 2018 (Build ID: 2017_11_07-07.51.41 127140 © Dassault Systemes, 2017).

4.3 Methods

The modeling and simulation were carried out in the following steps;

4.3.1 Laminate Modeling

The model was rectangular in shape, measuring 120 mm wide by 120 mm high, with a first phase thickness of 10 mm and a second phase thickness of 13 mm. The BMG material was sandwiched between the mild steel and the dyneema composites in the front layer, which was made of mild steel. First phase thicknesses were 5:2:3, second phase thicknesses were 5:3:5, and third phase thicknesses were 6:3:4. Four fully clamped boundary constraints were used to the armour plate design. The behavior of mild steel was predicted using the Johnson-Cook plasticity model, and the damage to the composite made of dyneema fibers was predicted using the Hashin damage model.

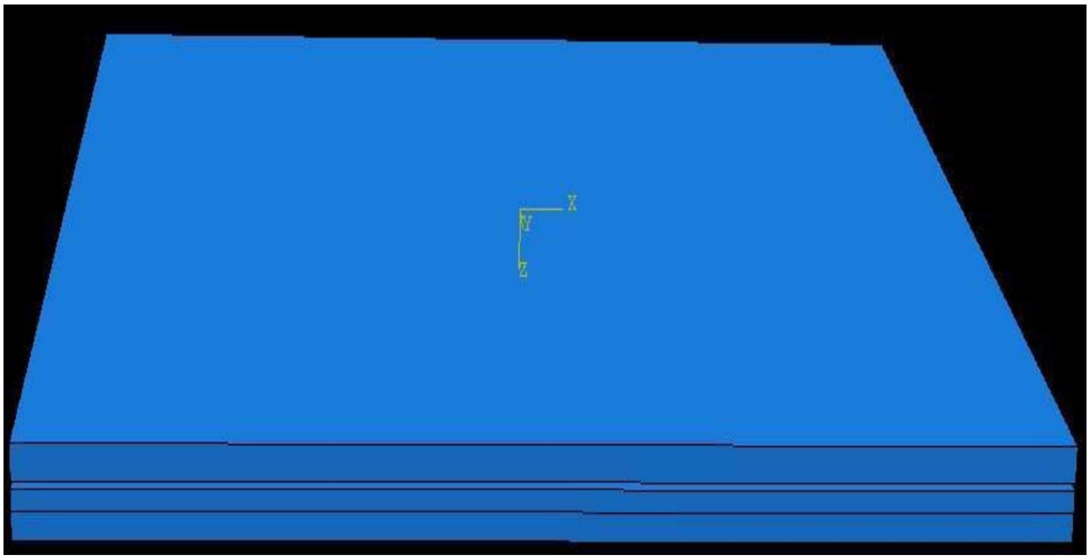

Figure 1: Mild steel, BMG and Dyneema stacking

4.3.2 Projectile Model

The 7.62mm APM2 bullet is made up of a lead element in the nose, a lead base filler, a metal jacket that glides, and a highly durable steel core [17]. In this study, an ogival-nosed bullet with a steel core that was assumed to be hardened 4340 steel was used, with the steel core of the 7.62mm APM2 bullet serving as the model for geometry and mass.

The eight-node hexahedral element C3D8R was used to mesh the projectile. The constitutive model used to represent the bullet's material behavior was the Johnson-Cook plasticity model. When metallic materials are subjected to high velocity impact and high strain rate, this model is widely used to predict the material reaction [17].

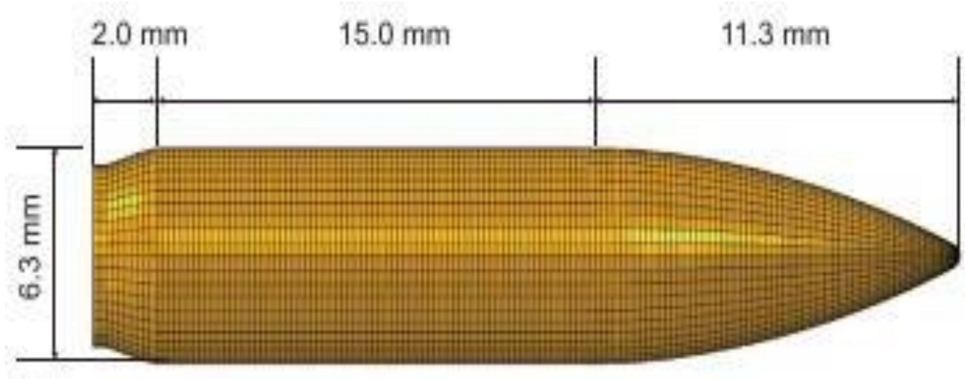

Figure 2: Finite Element Model of the Projectile and Dimensions [17]

In the first phase, the projectile was given beginning velocities of (275, 264, 249, and 215) m/s. These velocities were then raised until the material's ballistic limit was reached, at which point they were stopped. The Kinematic Contact algorithm was used to model the contact between the projectile and target. The target's contact surface was regarded as the slave surface and the projectile as the master. Hard contact was specified in the normal direction, and the effect of friction was given a value of 0.3 in the tangential direction. To discretize the projectile, hexahedral components with fixed sizes of 0.0005 were utilized.

5.0 RESULTS AND DISCUSSION

5.1 Results

A selection of results obtained for the simulation of the effects of projectile speed and different thicknesses of plates are given in Fig. 3 through Fig. 13 below and summarized in Table 3 and Figure 14 through 15;

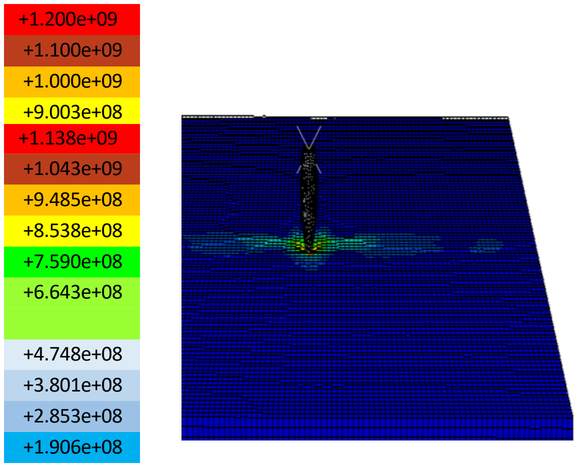

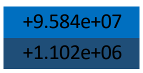

Figure 3: Von Mises stress at Impact (275m/s)

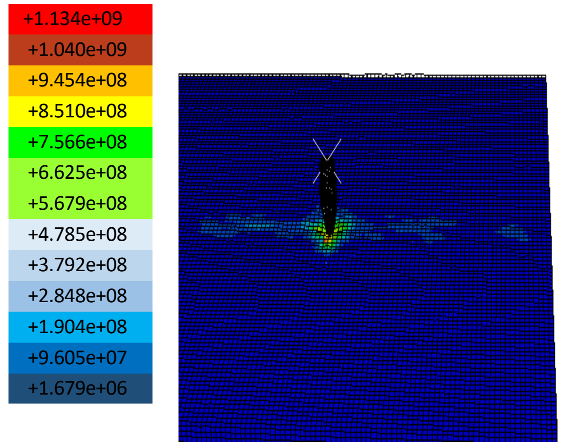

Figure 5: Von Mises stress at Impact (249m/s)

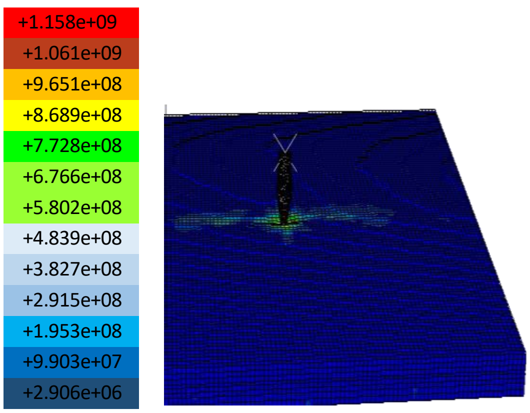

Figure 4: Von Mises stress at Impact (264m/s)

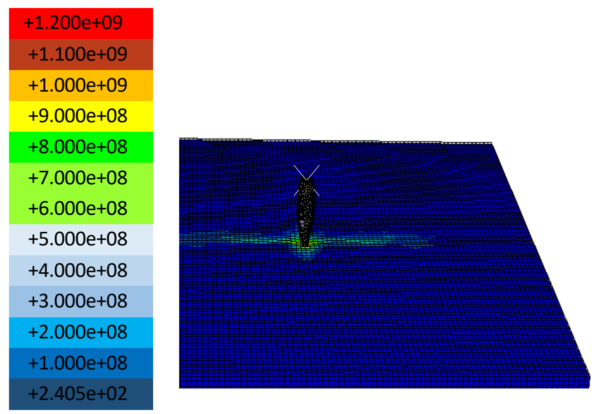

Figure 6: Von Mises stress at Impact (215m/s)

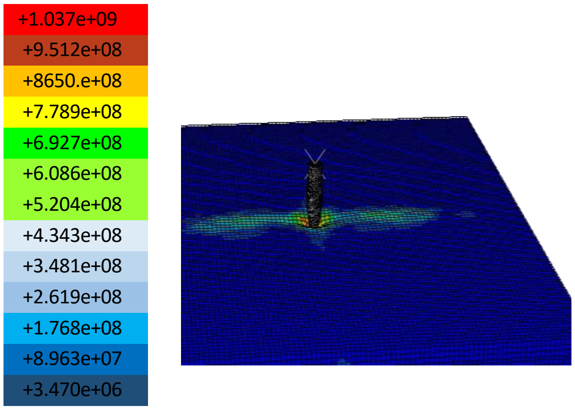

Figure 7: Von Mises stress at 400m/s (5:3:5 combination)

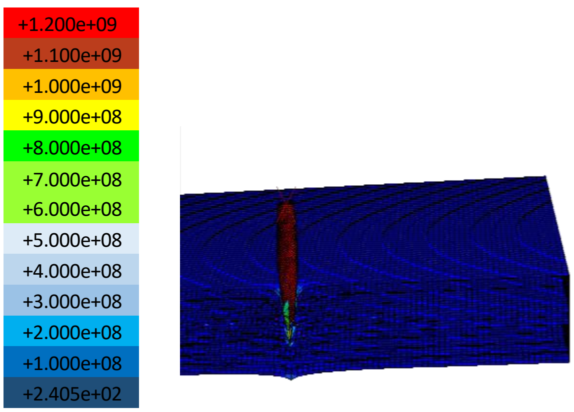

Figure 8: Von Mises stress at 500m/s (5:3:5 combination)

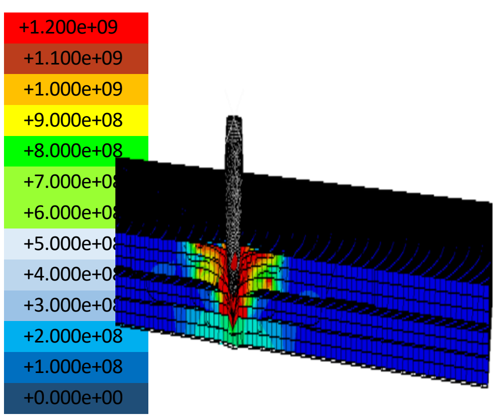

Figure 9: View cut of Von Mises stress at 800m/s (6:3:4 combination)

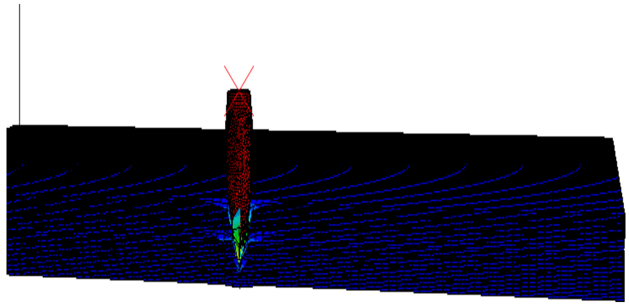

Figure 10: View cut of deflection at 800m/s (6:3:4 combination)

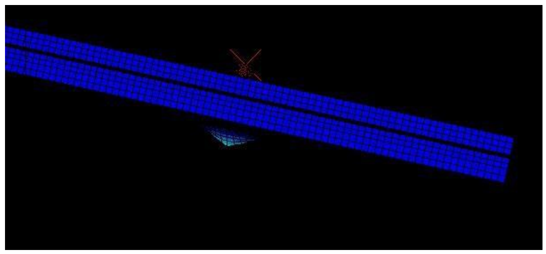

Figure 11: Simulation at 900m/s (6:3:4 combination)

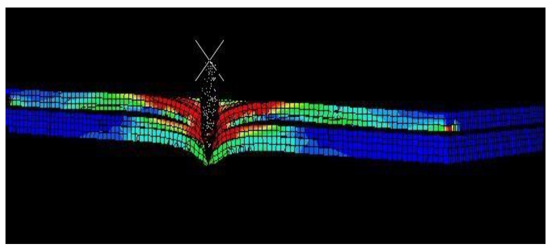

Figure 12: View cut of projectile and target at 900m/s (6:3:4 combination)

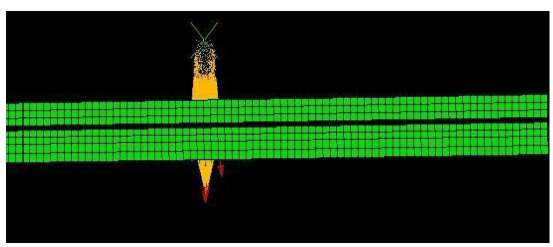

Figure 13: Complete perforation at 950m/s

5.2 Discussion of Results

The results obtained for the simulation of the effects of projectile speed on the target material of 10mm thickness are summarized in Table 3, Figure 14 and 15.

Table 3: Velocities with Corresponding Von Mises Stresses and Deflections for 10mm Thick Plate

S/No.	Velocity (ms)	Von Mises (N/m^2)	Deflection (m)
1	275	9.003×10^8	0.00080
2	264	8.689×10^8	0.00078
3	249	8.538×10^8	0.00074
4	215	8.510×10^8	0.00068

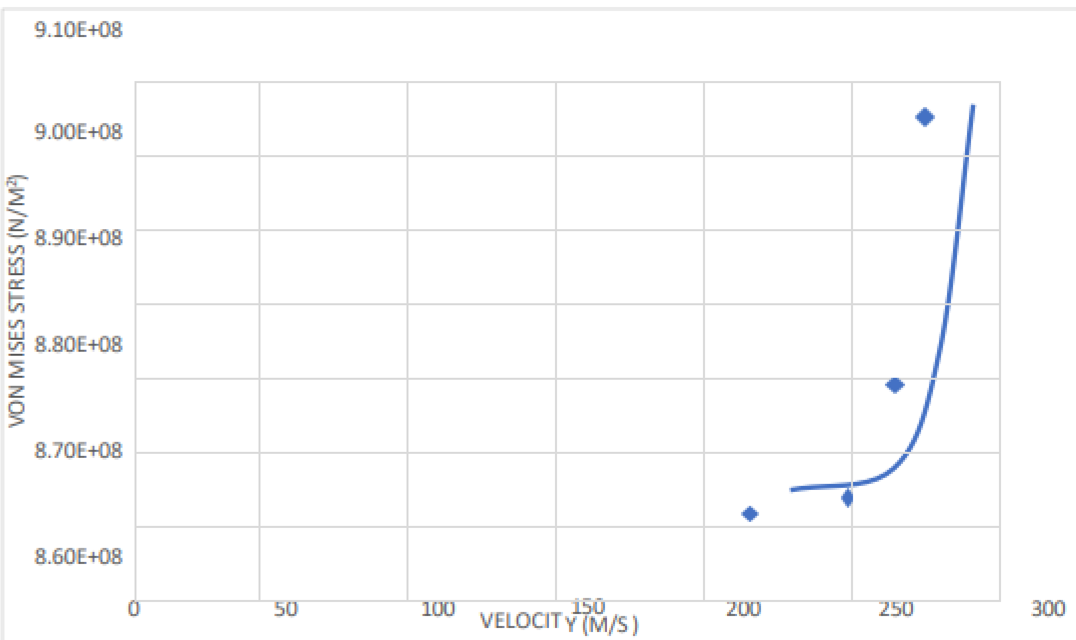

Figure 14: Plot of Von Mises Stress against Impact Velocity

The plot in Figure 14 shows the relationship between the impact velocity and the Von Mises stress. At an impact velocity of 275m/s, the Von Mises stress is given as $9.003 \times 10^8 N/m^2$. At impact velocity of 264m/s, the Von Mises stress is seen to decrease to $8.689 \times 10^8 N/m^2$. With the impact velocity at 249m/s, the corresponding Von Mises stress is $8.538 \times 10^8 N/m^2$. The Von Mises stress for impact velocity of 215m/s is given as $8.510 \times 10^8 N/m^2$.

Based on the simulation results, the Von Mises stress values increase as the velocity of the projectile increases. This trend is expected since higher velocities lead to greater kinetic energy and momentum, resulting in more forceful impacts. This agrees with the research findings of Li et al [23] and Weihong et al [24].

Very high Von Mises stresses suggest that the target material will experience significant deformation and potential failure under the impact conditions simulated. Depending on the specific material and application, such high levels of stress may be considered unacceptable or require additional design considerations to ensure safe and reliable performance. Generally, the NIJ standard-0101.06 for body armour requires that the armour material must be capable of withstanding a minimum of 2.4 x $10^9 N/m^2$ without failing [25].

It is also worth noting that the increase in Von Mises stress is not linear, as evidenced by the differences in the stress value for each velocity. The nonlinear relationship is likely due to various factors, such as the deformation characteristics of the target material, the geometry and velocity of the projectile, etc.

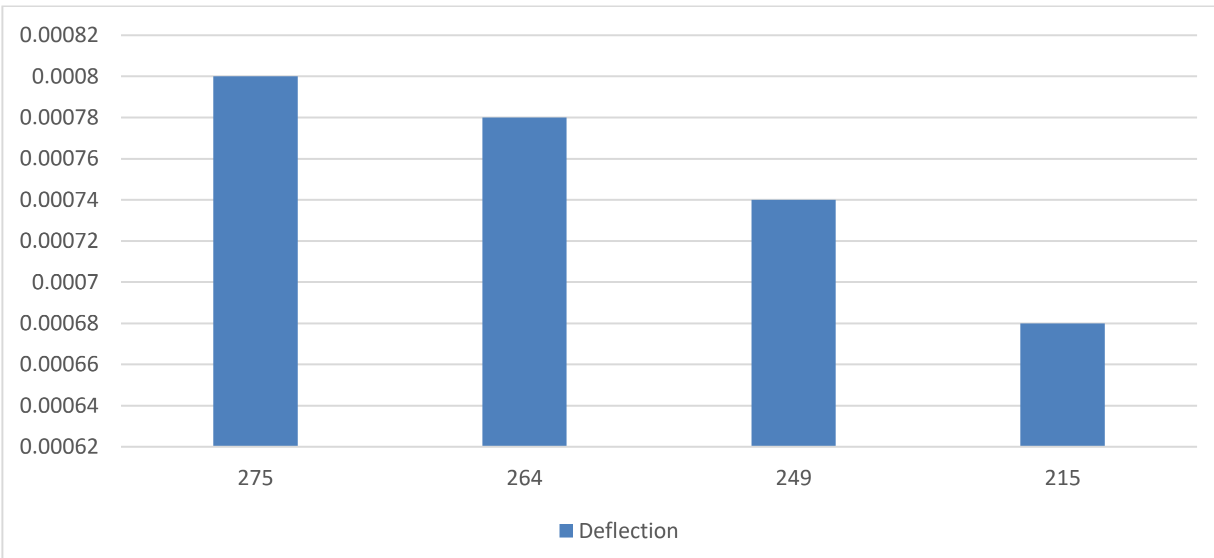

Figure 15: Chart of Deflection against Impact Velocity (10mm Plate Thickness)

Figure 15 shows the effect of the impact velocity on the target deflection. At an impact velocity of 275m/s, the deflection is shown to be 0.0008m. At impact velocity of 264m/s, the deflection value is 0.00078m. When the impact velocity is 249m/s, the deflection is shown to be 0.00074m and at an impact velocity of 215m/s, the deflection value is seen to be 0.00068m.

From the result obtained, the deflection increases with a corresponding increase in impact velocity. This could be due to the fact that as the velocity of the projectile increases, its kinetic energy increases. When the projectile hits the target, this energy is transferred to the target, causing it to deform and deflect. As the kinetic energy of the projectile increases, the amount of energy transferred to the target increases, which can result in a greater deflection. This is in good agreement with the research works of Wang et al [26] and

Weidong et al [27].

The results for the impact velocity of the projectile at normal, against the target material of thickness 13mm, in other to determine its ballistic limit are reflected in Table 4 and Figure 16.

Table 4: The Impact Velocity against the Deflection Values for 13mm Thick Plate

S/No.	Impact Velocity(m/s)	Deflection(m)
1	400	$1.084e^{-3}$
2	450	$1.108e\text{-}^{3}$
3	500	$1.131e\text{-}^{3}$
4	600	$1.181e\text{-}^{3}$
5	700	$1.193e\text{-}^{3}$
6	800	$1.194e\text{-}^{3}$
7	900	Noticeable bulge
8	950	Complete perforation

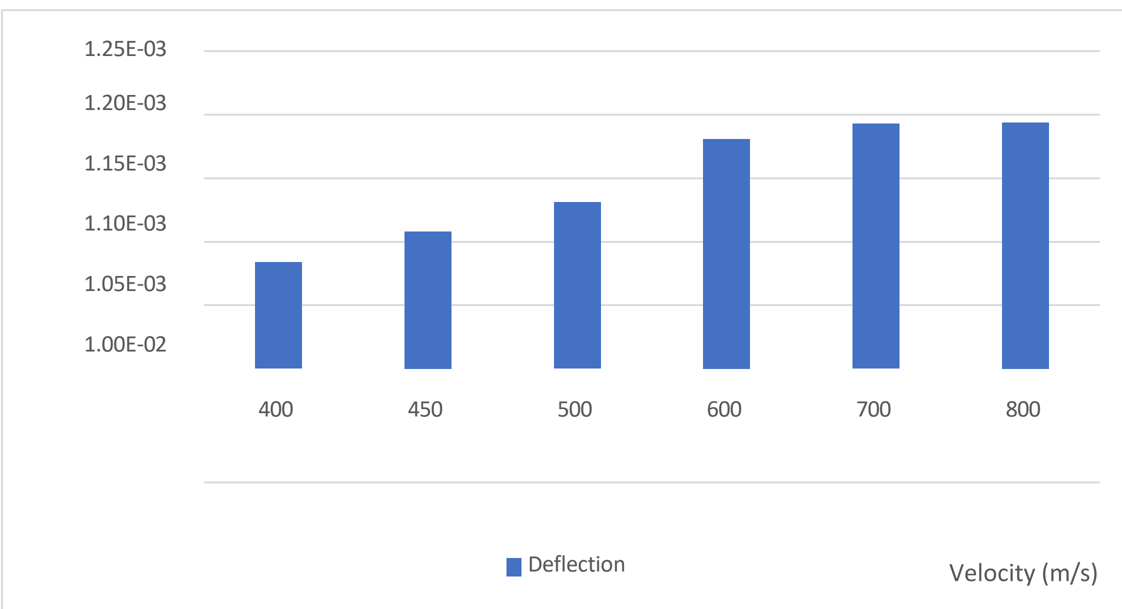

Figure 16: Chart of Deflection against Impact Velocity (13mm plate thickness)

Table 4 and Figure 16 show the trend that the increasing impact projectile velocity brings about a corresponding increasing deflection in the target material.
At impact velocity of 900m/s, a noticeable bulge (Figure 11 and 12) is seen at the backing plate and complete perforation (Figure 13) occurs at impact velocity of 950m/s, pegging the ballistic limit of the material of thickness 13mm at 850m/s. The bulge in the backing plate in Figure 11 can lead to injuries in the form of blunt trauma to the wearer. Though in some cases, bulging in armour plates can be permitted as long as it doesn't compromise the overall protective capability of the material, but perforation (Figure 13) is considered the most serious failure mode for ballistic materials.

6.0 CONCLUSION AND RECOMMENDATIONS

6.1 Conclusion

In the research, laminate composite materials were modeled and virtually tested for usage as ballistic protection. Using Abaqus Explicit FEA software for the numerical study, mild steel, bulk metallic glass, and dyneema were employed as the target laminate materials and tested against 7.62 API bullets. From the work, the following conclusions were made:

i. The modeling and simulation of the laminate composite material for use as body armour was carried out using the Abaqus Finite Element Analysis software, employing the Johnson-Cook constitutive models and the Hashin damage criteria for the modeling and simulation. The research showed that the combination is suitable for resisting the impact of 7.62mm API projectiles.

ii. The target was able to withstand impact from the projectile up to a velocity of 900m/s with a noticeable bulge in the back face of the target. The material was completely perforated at 950m/s, pegging the ballistic limit of the combination at 850m/s.

It is proposed that a minimum thickness of 14 mm, a combination of 6:3:5 be used in the design of the armour material. This is due to the fact that the probability of stopping a projectile increases with an increase in thickness of the material which would also improve the ballistic limit, which agrees with the findings of Senthil et al [28], Zaid and Travit [29].

6.2 Recommendations

The following suggestions are given for further studies;

1) The effect of multiple hits on the target should be investigated.

2) The design of a honeycomb structure from the hybrid material and its ballistic potentials as compared to the plain design should be investigated.

REFERENCES

[1] Ballistic Resistance of Personal Body Armour NIJ Standard–0101.04 (2008); U.S. Department of Justice. Office of Justice Programs. National Institute of Justice.

[2] Ashok, B. (2006); Lightweight Ballistic Composites. Woodhead Publishing Limited England; 73-77.

[3] Laible, R C. (1980); "Ballistic Materials and Penetration Mechanics. Methods and Phenomena, their Applications in Science and Technology". Volume 5. Elsevier Scientific Publishing Company.

[4] Handbook of Technical Textiles, (Second Edition) (2016); Volume 2: Technical Textile Applications (2016), Pages 193-236.

[5] "Ballistic Properties of Steel", The Balance Small Business, accessed April 30, 2023,https://www.thebalancesmb.com/ballistic-properties-of-steel-2340059.

[6] Haseeb A, Wahab M. A, and Syed S. A. R (2018); "Ballistic performance of bulk metallic glass composite plates," Journal of Composite Materials 52, no. 30: 4061-4071.

[7] Song J and Sun X (2012); "Numerical simulation of high-velocity impact on composite laminates using Abaqus/Explicit," Composite Structures 94, no. 9: 2848-2858.

[8] Bandyopadhyay A and Talreja R (2007); "Modeling and simulation of impact on composite materials using Abaqus/Explicit," Composites Part B: Engineering 38, no. 2: 231-238.

[9] Slepyan L. I. and Ayzenber-Stepanenko M. V. (1998); "Penetration of Metal-Fabrics Composites by Small Projectiles". The Institute for Industrial Mathematics. Beer-sheva 84105, Israel.

[10] Vemuri Madhu, Ramanjaneyulu K, Balakrishna Bhat T and Gupta N. K (2005); "An Experimental Study of Penetration Resistance of Ceramic Armour Subjected to Projectile Impact". International Journal of Impact Engineering. (p): 337-350.

[11] Kumar S, Durga S. G, Inderdeep S and Apurbba S (2009); "Behaviour of Kevlar/Epoxy Composite Plates under Ballistic Impact". Journal of Reinforced Plastics and Composites. Doi 10.1177/0731684409343727.

[12] Durmus A, Guden M, Gulcimen B, Ulku S and Musai E (2011); "Experimental Investigations on the Ballistic Performances of Cold Rolled Sheet Metals". Materials and Design 32 (1356-1366).

[13] Mohamed A and Ahmed F. (2014); "Mild Steel Plates Impacted by Hard Projectiles". Journal of Constructional Steel Research (99), pp. 57-71.

[14] Sanusi O. M. and Akindapo J. O. (2015); "Ballistic Performance of a Quenched and Tempered Steel against 7.62mm Calibre Projectile". Nigerian Journal of Technology. Vol. 34, P. 309-313.

[15] Chang C. S, Rao N. S. V. K and Mariappan M (2017); "Finite Element Modelling of Four Edges Simply Supported Steel Plate Under Impact Load". International Journal of Advanced and Applied Sciences 9(3S), pp. 257-278.

[16] Chanyoung Park and Chongdu Cho (2017); "Effect of High Hardness Armour Plate Sequences on Ballistic Impact Response". Journal of the Korean Society for Precision Engineering 34(6), pp. 417-424.

[17] Guodong G, Shah A and Larry D. P (2020); "Numerical Analysis of Ballistic Impact Performance of Two Ceramic-Based Armour Structures". Composites Part C: Open Access 3 (100061).

[18] Johnson G. R. and Cook V. H. (1993); "Lagrangian EPIC Code Computations for Oblique, Yawed-Rod Impact onto Thin-plate and Space-plate Targets at Various Velocities". International Journal of Impact Engineering. Volume 14, P. 373-383.

[19] Ballistic Test for Armour (1984): Military standard MIL-STD-662D. U.S Army Materials and Mechanics Research Center, Watertown, MA 02172.

[20] Senthil K, Iqbal M. A and Gupta N. K (2017); "Ballistic Resistance of Mild Steel Plates of Various Thicknesses against 7.62 AP Projectiles". International Journal of Protective Structures. (P): 1 – 22.

[21] Adamant Namiki Precision Jewel Company Limited (2022), accessed on 17th February 2022. https://www.ad-na.com/en/product/jewel/material/bmg.html

[22] Dyneema-Avient (2019), accessed on 25th April, 2022. https://www.dsm.com/dyneema/en_GB/home.html.

[23] Li Q, Erdong W, Ruyang Y, Quantian L, Gang L and Guangyong S (2022); "High-temperature and Dynamic Michanical Characterization of Closed-cell Aluminium Foams". International Journal of Mechanical Sciences. Vol. 230, 107548.

[24] Weihong H, Feng Z, Guoxing L and Dai-Ning F (2010); "Ballistic Impact Experiments of Metallic Sandwich Panels with Aluminium Foam Core". International Journal of Impact Engineering, 37(10): 1045-1055.

[25] National Institute of Justice Standard-0101.06 (2001).

[26] Wang N, Shilang X and Xinhua G (2011); "Experimental Study on Two-way Simply Supported Concrete Slab with Post-poured UHTCC under Concentrated Load". China Civil Engineering Journal, 44(8): 33-41.

[27] Weidong L, Lu W, weiqing L and Jianjin W (2016); "Behaviour of Glulam Columns Reinforced by Near-surface-mounted CFRP Laminates under Eccentric Compression Loading". Journal of Structural Engineering, 142(11): 04016109.

[28] Senthil K, Rupali S and Iqbal M. A (2017); "Finite Element Studies on Metal Plates against Oblique Impact of Cylindro-Conical Projectiles". 8th International Conference on Structural Engineering and Construction Management.

[29] Zaid A. I. O and Travis F. W (2003); "An Examination of the Effect of Target Thickness in the Perforation of Mild Steel Plate by a Flat-ended Projectile". International Journal of Mechanical Sciences. Vol. 16, Issue 6, P. 373 – 380.